Biocompatible β–chitin Hydrogel/Nanobioactive Glass Ceramic Nanocomposite Scaffolds for Periodontal Bone Regeneration

S. Sowmya[a], P.T. Sudheesh Kumar[a], K.P. Chennazhi[a], S.V. Nair[a], H. Tamura[b], R. Jayakumar[a*]

[a]Amrita Centre for Nanosciences and Molecular Medicine, Amrita Institute of Medical Sciences and Research Centre, Amrita Vishwa Vidyapeetham University, Kochi–682 041, India
[b]Faculty of Chemistry, Materials and Bioengineering, Kansai University, Osaka 564–8680, Japan
*Corresponding author: rjayakumar@aims.amrita.edu (R. Jayakumar).

Periodontal disease involves destruction of alveolar bone around the teeth leading to defects or rather loss of the tooth if left untreated. In most cases, tissue regeneration does not happen spontaneously which calls for interventional therapy with bone substitutes. Bone grafts and guided tissue regeneration (GTR) and are the most common approaches. However, the success rate is variable because of high susceptibility to infection and immunologic response which limits the clinical improvement. Realizing the vital role of synthetic biomaterials with limited immune response and good biological activity, we developed a nanocomposite scaffold using β–chitin hydrogel with bioactive glass ceramic nanoparticles (nBGC) by lyophilization technique. The prepared nanoparticles and nanocomposite scaffolds were characterized using FT–IR, XRD, DLS, TGA, AFM and SEM. Further, the porosity, swelling, *in vitro* degradation and biomineralization, cyto–toxicity, cell attachment and cell proliferation were also evaluated. The β–chitin/nBGC composite scaffolds were found to have enhanced porosity, swelling, bioactivity and degradation in comparison to the control scaffolds. The composite scaffolds were non–toxic to human osteosarcoma (MG63) and human primary osteoblasts (POB) cells and supported cell attachment, spreading and proliferation. The β–chitin/nBGC composite scaffolds were found to be satisfactory in all aspects, and these nanocomposite scaffolds could be promising candidates for the treatment of periodontal bone defects.

Introduction

Periodontal diseases are associated with gingival lesions, attachment loss and alveolar bone destruction. As a result roots of the teeth are exposed and tooth loss may occur. Periodontal diseases mostly require long–term periodontal treatment. One of the major goals of periodontal therapy is to obtain regeneration of the affected tissues with natural architecture and function [1–3]. Bone replacement grafts may be categorized as osteogenic, osteoinductive and osteoconductive. In general, grafts can be categorized into autogenous, allograft, alloplast and xenograft sources. Guided Bone Regeneration (GBR) and Guided Tissue Regeneration (GTR) can also achieve periodontal regeneration. GBR and GTR are surgical procedures commonly performed in the maxillo–facial region that utilize a barrier membrane to prevent epithelial migration and direct growth of hard and soft tissue into defective areas [4]. However the success rate of these techniques is variable because of high susceptibility to infection which results in limited clinical improvement. Thus tissue engineering may potentially provide an alternative solution [5, 6]. Various synthetic and natural biopolymers are used to construct scaffolds for tissue engineering applications. Biopolymers have an advantage of being biodegradable and these materials contain structural groups similar to natural extracellular components. These include synthetic polymers like poly(caprolactone), poly(lactic–co–glycolic acid), poly(ethylene glycol), poly(vinyl alcohol), polyurethane and natural polymers like alginate, collagen, gelatin, chitin, chitosan etc. Among these, chitin and chitosan have shown tremendous promise as tissue supporting materials [7, 8].

Chitin is a biopolymer composed of N–acetyl D–glucosamine units linked by β–1, 4 glycosidic bonds. Chitin is extensively acetylated and insoluble in water and acid due to its rigid crystalline structure supported by hydrogen bonds [9, 10]. Chitin is known to be a biodegradable polymer in nature because the β–1, 4–glycosidic linkage is susceptible to degradation by lysozyme. Due to its non toxic nature, chitin is useful for a variety of biomedical applications. Depending on source, there are mainly three polymorphic forms of chitin– α–chitin, β–chitin and γ–chitin. β–chitin is present in squid pen. In β–chitin all chains are aligned in parallel manner [9, 11, 12]. Chitin hydrogels are an appealing scaffold material because they are structurally similar to the extracellular matrix of many tissues that can be easily processed and delivered in a minimally invasive manner and hence are ideal for periodontal applications [13–15]. The calcium solvent

system was found to be a good solvent to prepare chitin hydrogel. [16].Hydrogels contain 90% water and have typical mechanical properties. They can be spontaneously colonized by blood and favor the migration of the cells responsible for the bone healing [17].

One of the most popular materials used for bone repair is synthetic hydroxyapatite (HAp). However they have very slow rates of resorption and are hence used for bone augmentation and not regeneration. Bioactive glasses can serve as alternatives to HAp. Bioactive glasses have been used for the past three decades since the discovery of Bioglass by Larry Hench [18]. Due to their good bioactivity, osteoinductivity and biodegradability, bioactive glasses are being used as bone repair materials [19] and form a bond to bone faster than other bioactive ceramics due to formation of carbonated apatite layer on their surface in physiological fluid. Bioactive glass has a unique ability to bond to both hard and soft tissue. These nanoceramics provide alternatives for orthopaedic and dental applications. Bioactive glasses are superior to HAp as they serve two purposes: improve the osseointegration of implants; protect the metal against corrosion from the body fluids and the tissue from corrosion products of the alloys [20, 21]. They prevent the formation of fibrous tissue at the prosthesis–bone interface and favour a strong chemical bond between implant and tissue [22]. Bioactive glasses have been reported to promote and increase cellular adhesion, enhance osteoblast proliferation and differentiation and an increase in biomineralization process. It has also been reported that bioactive glass could directly influence gene expression of osteoblasts [19]. Sol–gel technique is a low temperature preparation method. The sol–gel process allows one to obtain glasses of higher purity, surface area, and homogeneity than by the fusion method [23]. Hence, due to the advantages of these materials, we synthesized and studied in detail about β–chitin hydrogel/nBGC composite scaffolds for periodontal bone applications.

Materials and Methods

Chitin was received from KYOWA TECNOS Co. Ltd.(Tiba,Japan) as powder. Sodium hydroxide, Triton–X 100, Nitric acid, Ammonia were purchased from Qualigens Fine chemicals, India. Tetraethyl orthosilicate (TEOS), Calcium Nitrate (Ca(NO$_3$)$_2$.4H$_2$O), Ammonium dibasic phosphate, Polyethylene glycol, Calcium Chloride, Methanol, Minimum essential medium (MEM), Acetic acid, Paraformaldehyde were purchased from SIGMA Aldrich Company, Glutaraldehyde and Hen Lysozyme were purchased from Fluka. DAPI, Alamar Blue, Trypsin–EDTA and Fetal Bovine Serum (FBS) were obtained from Gibco, Invitrogen Corporation. MG–63 was obtained from NCCS, Pune, India. Osteoblast growth media and POB were obtained from PromoCell. *Streptococcus Aureus* (ATCC 25923) and *Escherichia Coli* (ATCC 25922) strains were obtained from Microbiology lab of Amrita Institute of Medical Sciences, Kochi, India.

Preparation of β–chitin Hydrogel

β–chitin hydrogel was prepared according to the literature [15]. β–chitin was added to a mixture of saturated CaCl$_2$.2H$_2$O /methanol solvent to prepare 0.5 w/v chitin hydrogel. This mixture was allowed to stir till a transparent chitin solution was obtained and later the undissolved chitin was removed by filtration. This was followed by addition of water (to break the bond between chitin and CaCl$_2$) and the solution was stirred for 2hrs. Then the hydrogel was kept aside undisturbed for a day following which the water (containing CaCl$_2$) was removed by suction filtration. The hydrogel was then dialyzed against distilled water for 2 days to remove the impurities, methanol and remaining CaCl$_2$.

Preparation of nBGC

For preparing nBGC, first, 7.8 g of TEOS and 12.5 g of Ca(NO$_3$)$_2$.4H$_2$O were dissolved in a mixture of distilled water and ethanol (120 ml:40 ml) and stirred at room temperature for the hydrolysis of TEOS until a transparent solution was obtained. The pH value of this solution was adjusted to 2 with HNO$_3$. Secondly, 1.98 g of NH$_4$H$_2$PO$_4$ was dissolved in 1500 ml of distilled water containing 15 g of PEG (20,000 MW) and the pH of the solution was adjusted to 10 with ammonia water. When TEOS was completely hydrolyzed in about 4 h, the TEOS–Ca(NO$_3$)$_2$ solution was dropped into NH$_4$H$_2$PO$_4$ solution under vigorous stirring and the reaction mixture aged for 24 h at room temperature to obtain a white gel precipitate. Finally, CaO–SiO$_2$-P$_2$O$_5$ ternary BGC nanoparticles were obtained by filtration, lyophilisation (CHRIST ALPHA 2–4 LD Plus) and calcination of the precipitate [24].

Preparation of β–chitin/nBGC Composite Scaffolds

β–chitin/nBGC composite scaffolds were prepared by adding different concentrations of nBGC into β–chitin hydrogel. 0.5 and 1% nBGC was added to 10g of β–chitin hydrogel, stirred well for 2 hrs. Then the hydrogel was transferred into a 24 well culture plate and pre–freezed for 12hrs followed by lyophilization at –80ºC to obtain β–chitin/nBGC composite scaffolds.

Characterization Studies

β–chitin was characterized using X–Ray Diffraction (PANalytical X'Pert PRO), FTIR (PerkinElmer Co, SPECTRUM RX1, FT–IR), Thermogravimetric Analysis (SII TG–DTA6200) instruments. The morphology and size of nBGC was characterized using Dynamic Light Scattering measurements (DLS–ZP /Particle Sizer Nicomp™ 380 ZLS, particle sizing system), Atomic Force Microscope (Jeol JSPM–5200) by dispersing in ethanol. XRD pattern of nBGC was characterized at room temperature using Panalytical Diffractometer (XPERT PRO powder). The structural morphology of chitin/nBGC composite scaffold was characterized by Scanning Electron Microscope (JEOL,JSM–6490LA, Japan). The samples were prepared by taking thin sections with a scalpel blade. The sections were platinum sputtered in vaccum (JEOL, JFC 1600, Japan). Energy–dispersive XRay Spectroscopy (EDS) analysis was performed on JEOL JSM 6490 LA. Thin section of scaffold was placed on carbon tape coated stub. The sample was then platinum coated with JEOL JFC 1600. The XRD patterns of the composite scaffolds were analysed at room temperature using Panalytical Diffractometer (XPERT PRO powder) (Cu Kα radiation) operating at a voltage of 40 kV. XRD were taken at an angle of 5–60° and the process parameters were: scan step size 0.02 (2θ) and

scan step time 0.05s. IR spectra of dried nBGC and composite scaffolds were characterized using FT–IR spectrometer (Perkin–Elmer RX1). nBGC and composite scaffolds were powdered and mixed thoroughly with potassium bromide and pelletized. The IR spectra of the prepared pellets were analysed at a range of 400–4000 cm^{-1}. Thermogravimetric Analysis of the composite scaffolds was carried out using TG/DTA instrument (SII TG–DTA6200).

Swelling Studies

The swelling studies were performed in PBS (pH 7.4) at 37°C [25]. The dry weight of three samples each of β–chitin scaffold (control) and β–chitin/nBGC composite scaffold were taken and noted as W_d. The scaffolds were then placed in PBS buffer solution (pH 7.4) at 37°C for different time durations such as 1, 3 and 7 days respectively. After the predetermined time, the scaffolds were taken out, the surface adsorbed water was removed by filter paper and wet weight was recorded as W_w. The ratio of swelling was determined using the Eq. (1):

$$\text{Swelling ratio} = (W_w - W_d)/W_d \qquad (1)$$

Swelling ratio was expressed as mean±SD (n = 3).

Porosity Studies

The porosity was determined by the liquid displacement method [25]. Three samples each of β–chitin scaffold (control) and β–chitin/nBGC composite scaffolds were immersed in 100% ethanol for 48 hrs until it was saturate, and the porosity of the sample was calculated according to the formula

$$P = (W_2 - W_1)/\rho V_1 \qquad (2)$$

where W_1 and W_2 represent the weight of the scaffolds before and after immersing in ethanol, respectively, and V_1 is the volume of scaffold before immersing, ρ is a constant of the density of ethanol. Porosity was expressed as mean±SD (n = 3).

In Vitro Degradation Studies

The degradation of the scaffold was studied in PBS (pH 7.4) medium containing lysozyme at 37°C. Three samples each of β–chitin scaffold (control) and β–chitin/nBGC composite scaffold were immersed in lysozyme (10,000 U/ml) containing medium and incubated at 37°C for 7, 14, 21 and 28 days respectively. Initial weight of the scaffold was noted as W_i. After soaking for 7, 14, 21 and 28 days, the scaffolds were removed from the solution and rinsed with deionised water to remove ions adsorbed on the surface and freeze dried [26]. The dry weight after lyophilisation was noted as W_t. The degradation of scaffold was calculated using Eq. (3):

$$\text{Degradation (Rate of weight loss \%)} = W_i - W_t / W_i \times 100 \% \qquad (3)$$

Degradation rate was recorded as mean±SD (n = 3).

In Vitro Biomineralization Studies

Three samples each of β–chitin scaffold (control) and β–chitin/nBGC composite scaffold of equal weight and shape were immersed in 1 X simulated body fluid (SBF) prepared according to literature [27] by adding NaCl (7.995g), KCl (0.224g), $CaCl_2.2H_2O$ (0.368g), $MgCl_2.6H_2O$ (0.305g), K_2HPO_4 (0.174g) $NaHCO_3$ (0.349g), and $Na_2SO_4.10H_2O$ (0.161g) to 1L of distilled water .The pH of the solution was then adjusted to 7.4 by the addition of Tris/HCl. The samples were incubated at 37°C in closed falcon tubes for 7, 14, 21 and 28 days. After the specified time periods, the scaffolds were removed and washed with deionised water to remove adsorbed minerals. Finally the scaffolds were lyophilized, sectioned and viewed using SEM and EDS for mineralization (n=3).

Cell Viability

Cell viability of the β–chitin scaffold and β–chitin/nBGC composite scaffolds were evaluated by indirect cell viability using Alamar Blue assay. Alamar blue reagent is a cell viability and cell proliferation indicator that uses the inherent reducing power of live cells as an indicator of metabolic activity. Assay incorporates a redox indicator that undergoes a colorimetric change in response to cellular metabolic reduction. The cell viability of composite scaffolds with different concentration of nBGC was done according to ISO 10993–5. Triplicates of each sample were taken and samples were UV sterilized for a day following which they were incubated in serum containing media in a shaker for 24hrs and 48hrs at 37°C (extraction ratio was 10mg:1ml, sample:media). 100μl of the extract was taken for the test. POB and MG63 cells were seeded into each well of a 96 well plate at a density of 1×10^4 cells/well and incubated. After 24 hrs, the media was replaced with the extract and again incubated for 24 hrs. After the incubation period of 24 hrs, extract was replaced with 100 μl of fresh media containing 10% of Alamar blue solution. After 4 hrs of incubation, the absorbance of the solution was measured at a wavelength of 570 and 600 nm using a Microplate reader (Biotek PowerWave XS, USA).

Cell Attachment

Cell attachment studies were conducted using MG–63 and POB. Cells were maintained in the cell culture facility in MEM with 10% FBS and 100 U/ml penicillin–streptomycin for MG63 and in Osteoblast Growth Media with 100 U/ml penicillin–streptomycin for POB cells. Cells were detached from the culture plate at 80–85% confluence and used for seeding on the β–chitin scaffold (control) and β–chitin/nBGC composite scaffold. Prior to cell seeding, scaffolds were sterilized using UV treatment and incubated with culture medium for 1 hr at 37°C in a humidified incubator with 5% CO_2 and 85% humidity. Then the culture medium was removed completely from the scaffolds. Cells were seeded drop wise onto the top of the scaffolds (1×10^5 cells/scaffold), which fully absorbed the media, allowing cells to distribute throughout the scaffolds. Subsequently, the cell–seeded scaffolds were kept at 37°C in a humidified incubator under standard culturing conditions for 12 hrs in order to allow the cells to attach to the scaffolds. After 4 hrs, the scaffolds were fed with additional culture medium. After 12 hrs of incubation the scaffolds for SEM analysis were washed with PBS and fixed with 2.5 % glutaraldehyde for 1 hr following which the scaffolds were thoroughly washed with PBS and sequentially dehydrated in a graded ethanol series, air–dried, platinum sputtered in vacuum and examined using a scanning electron microscope.

For DAPI staining, the scaffolds were fixed with 4% Paraformaldehyde in PBS for 20 mins. Following this the scaffolds were washed with PBS and permeabilised with 0.5% Triton X–100 (in PBS) for exactly 5 mins. Then the scaffolds were blocked using 1% FBS (in PBS) and washed with PBS and stained with 50 µl DAPI (in PBS) and incubated in dark for 5 mins. Then the scaffolds were thoroughly washed with PBS and viewed under fluorescent microscope (Olympus–BX–51).

Cell Proliferation Studies

Cell proliferation studies were conducted similar to cell attachment studies using MG–63 and POB. The cell–seeded scaffolds were kept at 37°C in a humidified incubator under standard culturing conditions for 72 hrs in order to allow the cells to proliferate on the scaffolds. After 4, 12, 24 and 48 hrs, the scaffolds were fed with additional culture medium. After 72 hrs of incubation the scaffolds for SEM analysis were washed with PBS and fixed with 2.5% glutaraldehyde for 1 hr following which the scaffolds were thoroughly washed with PBS and sequentially dehydrated in a graded ethanol series, air–dried, platinum sputtered in vacuum and examined using a scanning electron microscope.

DAPI staining procedure was done similar to cell attachment. The scaffolds were thoroughly washed with PBS and viewed under fluorescent microscope.

POB Maturation and Mineralization

Osteoblast growth medium was supplemented with 50 U/ml penicillin and streptomycin prior to the commencement of the experiment. Prior to cell seeding, scaffolds were sterilized using UV treatment and incubated on a 24 well plate with the prepared culture medium for 1 h at 37°C in a humidified incubator with 5% CO_2 and 85% humidity. POB cells were seeded at a density of 1×10^4 cells/well and media was changed every 2–3 days for 7, 14 and 21 days. Cells were cultured without osteogenic supplements. The cell–seeded scaffolds were kept at 37°C in a humidified incubator under standard culturing conditions for the specified time periods. After 7, 14 and 21 days, the scaffold samples were washed with PBS and fixed with 2.5% glutaraldehyde for 1 hr following which the scaffolds were thoroughly washed with PBS and sequentially dehydrated in a graded ethanol series, air–dried, platinum sputtered

in vacuum and examined using a scanning electron microscope [28].

Statistical Analysis

All quantitative results were obtained from triplicate samples. Data was expressed as the mean±SD. Statistical analysis was carried out using Student's two–tailed t–test. A value of $p < 0.05$ was considered to be statistically significant.

Results

Characterization of nBGC

The particle size and morphology of nBGC was characterized using AFM (Fig. 1A) and DLS (Fig. 1B). The nBGC are spherical shaped and the size of the particles was in the range of 50–150 nm. The particle size distribution of nBGC showed an average size of 72 nm.

SEM Analysis

The surface morphology of β–chitin (control) and β–chitin/nBGC composite scaffolds is shown (Fig.2A). The scaffolds appear as porous structures with smooth surface morphology. The control scaffold is found to be more porous than the β–chitin/nBGC composite scaffold. The pore size of β–chitin/nBGC composite scaffold is in the range of 100–150 µm.

EDS Analysis

The EDS spectrum (Fig.2B) of β–chitin/nBGC composite scaffold shows the peaks of Ca, P, Si and O. The atomic ratio of Si:Ca:P:O was found to be 29:13:8:48 as determined by EDS.

FTIR Analysis

FTIR spectra of nBGC showed vibration bands at 467cm⁻¹ and a shoulder at 1200cm⁻¹ which are assigned to Si–O–Si bending mode. The vibration band at 1070cm⁻¹ and a double peak at 607 and 567cm⁻¹ are due to the stretching vibration of phosphate groups [11]. The peaks at 2889 and 1637cm⁻¹ are attributed to CH stretching and O–H (molecular water) bending vibration band of PEG. This indicates that the PEG is present on the surface of nBGC [29]. FT–IR spectra of β–chitin scaffold indicate the peaks
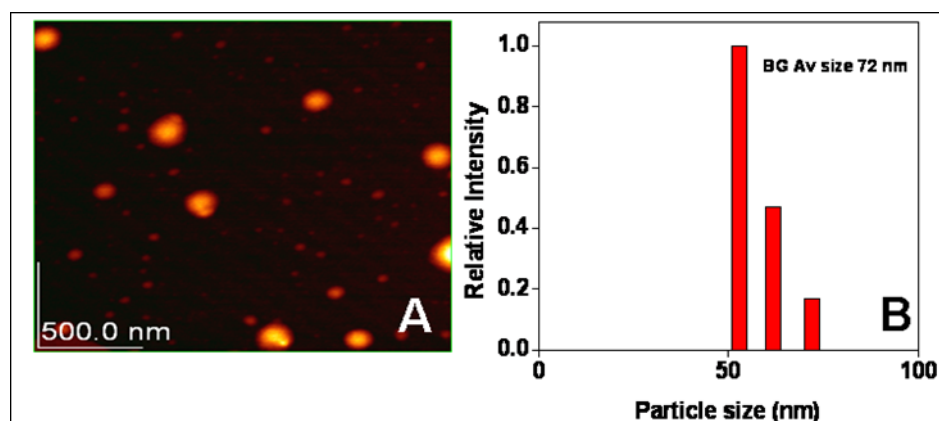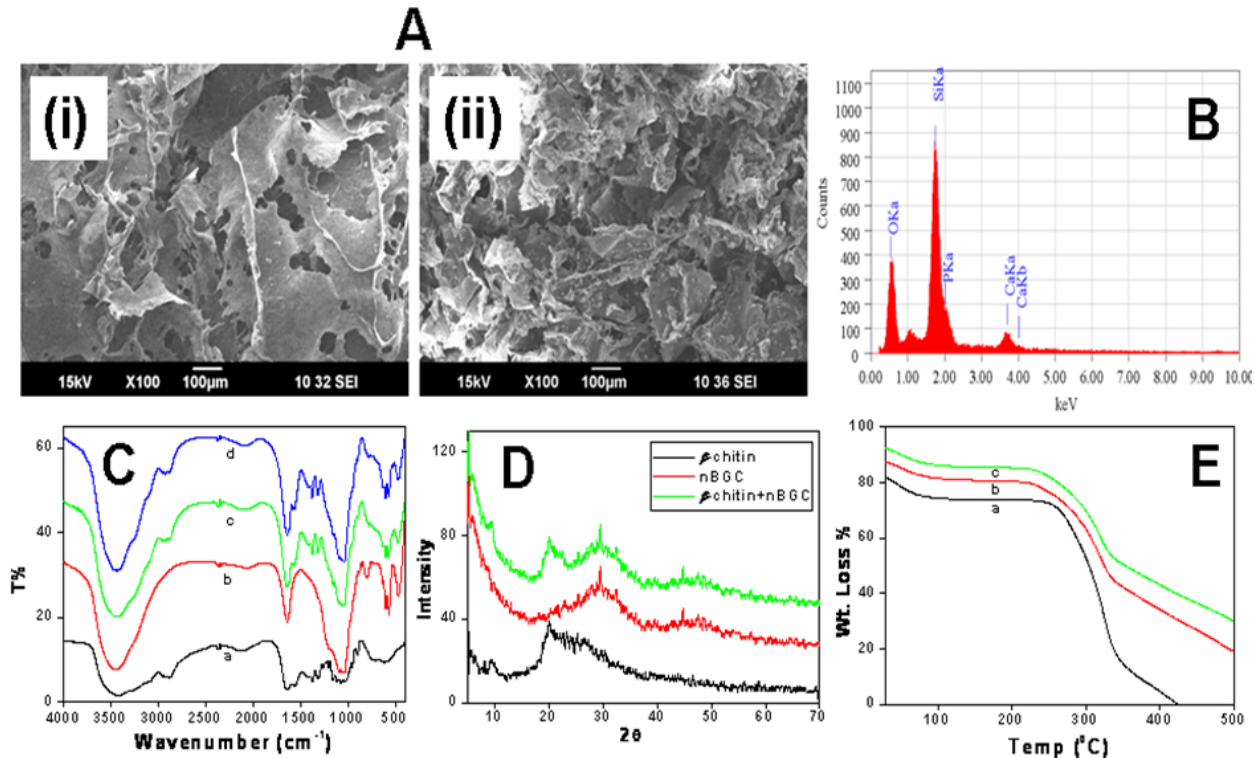

Figure 1: A. AFM image showing size and morphology of nBGC, B. Particle size distribution

Figure 2: SEM images showing macroporous structure of A. (i) *β*–chitin scaffold, and (ii) *β*–chitin/nBGC composite scaffold, with pore size ranging from 100–300 μm, B. EDS spectra of *β*–chitin/nBGC composite scaffold; C. FT–IR spectra of (i) *β*–chitin scaffold(control), (ii) nBGC, (iii) *β*–chitin/0.5% nBGC, (iv) *β*–chitin/1% nBGC composite scaffolds D. XRD spectra of (i) *β*–chitin scaffold(control), (ii) nBGC, (iii) *β*–chitin/nBGC scaffolds, E. TGA profile of (i) *β*–chitin scaffold(control), (ii) *β*–chitin/0.5% nBGC, (iii) *β*–chitin/1% nBGC composite scaffolds.

at 1231 and 1748 cm^{-1} which correspond to C–O and C=O stretching vibration modes of the amide group. For *β*–chitin the peaks at 1626 cm^{-1} correspond to amide I. [30]. FT–IR spectra of *β*–chitin/nBGC composite scaffolds showed the combined peaks of *β*–chitin and bioglass (Fig.2C).

XRD Analysis

The XRD spectra of *β*–chitin show peaks at 2θ =10.4 and 20.1°, which are the characteristic peaks of *β*-chitin [30, 31]. The XRD spectra of nBGC confirmed that the calcinated glass generally existed in amorphous state and no diffraction peaks could be observed except a broad band between 20 and 40° (2θ) [29] (Fig.2D).

Thermo Gravimetric Analysis

In the thermogram, all the scaffolds showed decomposition in the range of 50–100°C. This was due to the removal of physically adsorbed water. In the case of *β*–chitin control, it showed a second decomposition in the range of 270 to 350°C and composite scaffolds showed in the range of 270 to 370°C and it can be attributed to the decomposition of polysaccharide structure of *β*–chitin [30]. The decomposition rates of the composite scaffolds were increased slightly, due to presence of nBGC (Fig.2E).

Swelling Studies

The swelling behaviour of *β*–chitin scaffold (control) and *β*–chitin/nBGC composite scaffolds in PBS is shown (Fig.3A). nBGC incorporated scaffolds showed lower swelling compared to control. The swelling was increased with time till 7 days and thereafter the scaffolds began to degrade [31].

Porosity Studies

The porous nature of *β*–chitin scaffold (control) and *β*–chitin/nBGC composite scaffolds in absolute ethanol is shown (Fig.3B). nBGC incorporated scaffolds showed lesser porosity in comparison to control. This pore size of the scaffold was reduced due to presence of nBGC [24].

In Vitro Degradation Studies

The *in vitro* degradation profile of *β*–chitin scaffold (control) and *β*–chitin/nBGC composite scaffolds is shown (Fig.3C). *β*-chitin can be degraded by lysozyme enzyme present in human body. The results showed that *β*–chitin/nBGC composite scaffolds lose 20–25% of their weight after 28 days of incubation with lysozyme.

In Vitro Biomineralization Studies

The *in vitro* biomineralization of *β*–chitin scaffold (control) and *β*–chitin/nBGC composite scaffolds immersed in 1X SBF after 7, 14, 21 and 28 days. The SEM image of an apatite like layer on the surface of *β*–chitin/nBGC composite scaffold is shown (Fig.4A–D). EDS spectra of mineralization showed the Ca/P ratio of 1.71 (Fig.4E). This result shows the bioactive nature of the nanocomposite scaffolds [11].

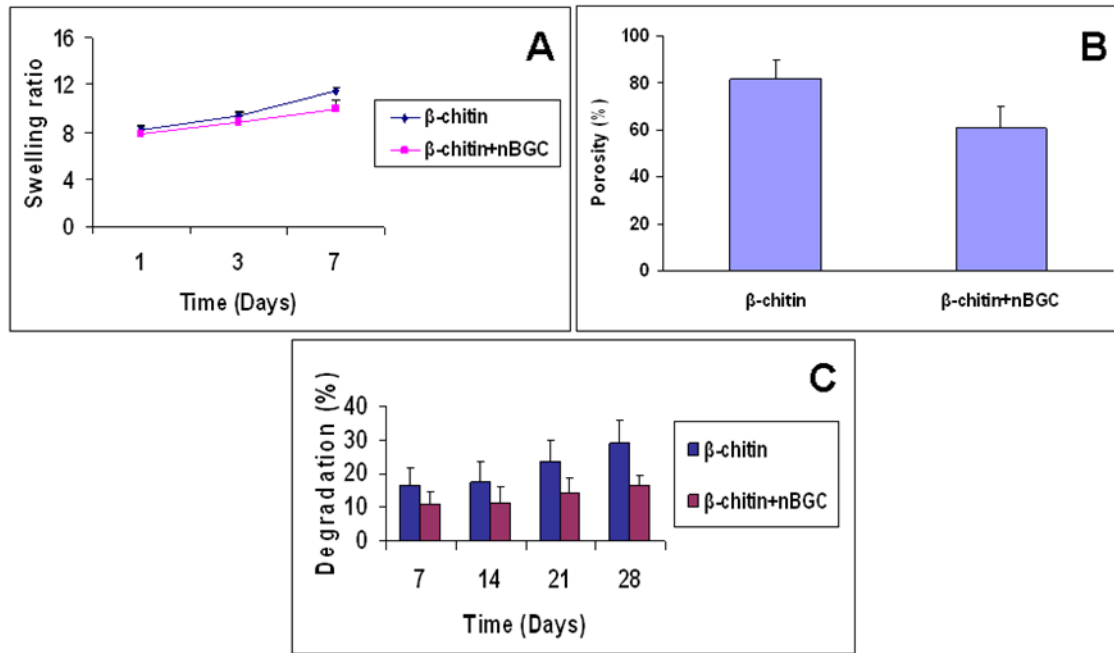The XRD studies of *β*–chitin/nBGC mineralized composite scaffolds showed sharp peaks at 26 and 31.7° (2θ)

Figure 3: A. Swelling studies of *β*–chitin scaffolds in PBS, B. Porosity studies of *β*–chitin scaffolds and C. *In–vitro* degradation profile of *β*–chitin scaffolds in PBS.
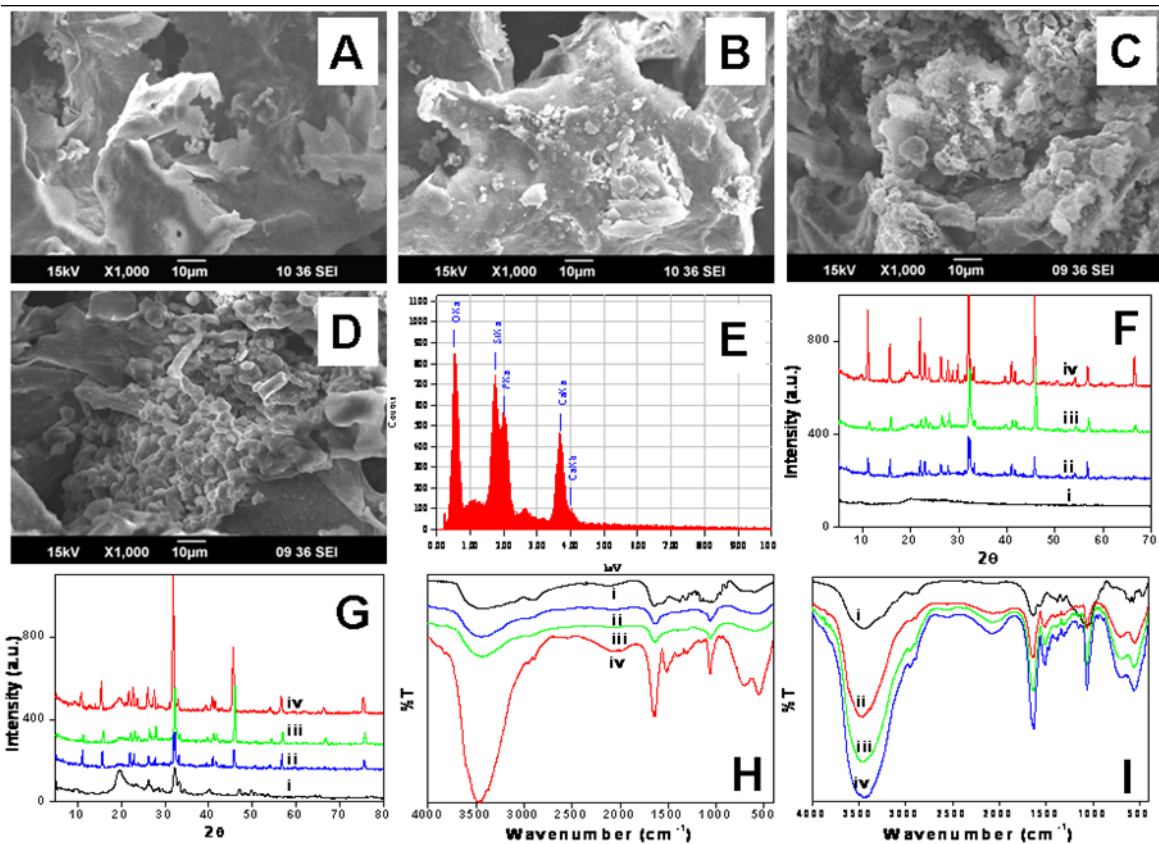

Figure 4: SEM images of in–*vitro* biomineralization of A. *β*–chitin (control) scaffold in SBF after 14 days and *β*–chitin/nBGC composite scaffold in SBF after B. 7 days, C. 14 days and D. 21 days. E. EDS spectra of in–*vitro* biomineralization in SBF of *β*–chitin/nBGC composite scaffold after 14 days. XRD spectra of in–*vitro* biomineralization in SBF, F. *β*–chitin (control) scaffold and G. *β*–chitin/nBGC composite scaffold after (i) 0, (ii) 7, (iii) 14 and (iv) 21 days. FTIR spectra of in–*vitro* biomineralization in SBF, H. *β*–chitin (control) scaffold and I. *β*–chitin/nBGC composite scaffold after (i) 0, (ii) 7, (iii) 14 and (iv) 21 days.
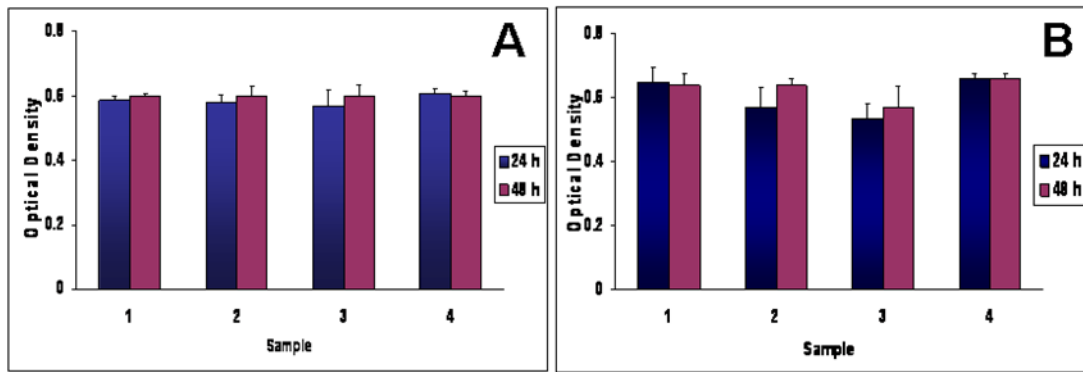
Figure 5: A. Cell Viability of β–chitin scaffold and β–chitin/nBGC composite scaffold for MG–63 cells using Alamar Blue assay (Samples: 1) β–chitin, 2) β–chitin/0.5% nBGC, 3) β–chitin/1% nBGC, 4) Positive Control–Media). B. Cell Viability of β–chitin scaffold and β–chitin/nBGC composite scaffold for POB cells using Alamar Blue assay (Samples: 1) β–chitin, 2) β–chitin/0.5% nBGC, 3) β–chitin/1% nBGC, 4) Positive Control–Media).

attributed to 211 plane of hydroxyapatite [25, 31] (Fig.4F, G). The XRD data clearly shows the increase in the intensity of peaks from 7–21days due to increased deposition of HAp with increased soaking time in SBF.

The FTIR studies of β–chitin/nBGC mineralized composite scaffolds showed sharpening of peaks at 603 and 567cm⁻¹

corresponding to stretching vibration bands of phosphate group and at 3570 cm⁻¹ attributed to –OH group [28] (Fig.4H,I). The FTIR spectra clearly indicates the sharp increase in the intensity of peaks from 7–21 days and deposition of HAp was found to increase with the increase of soaking time in SBF.
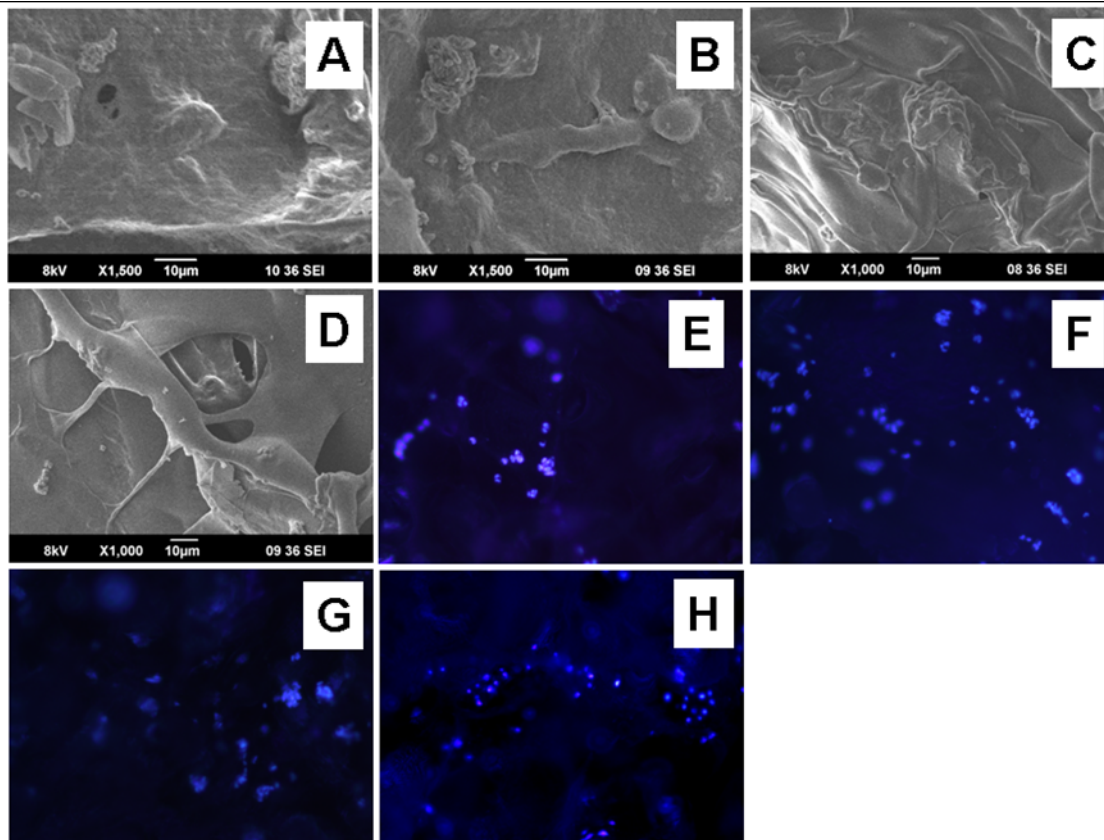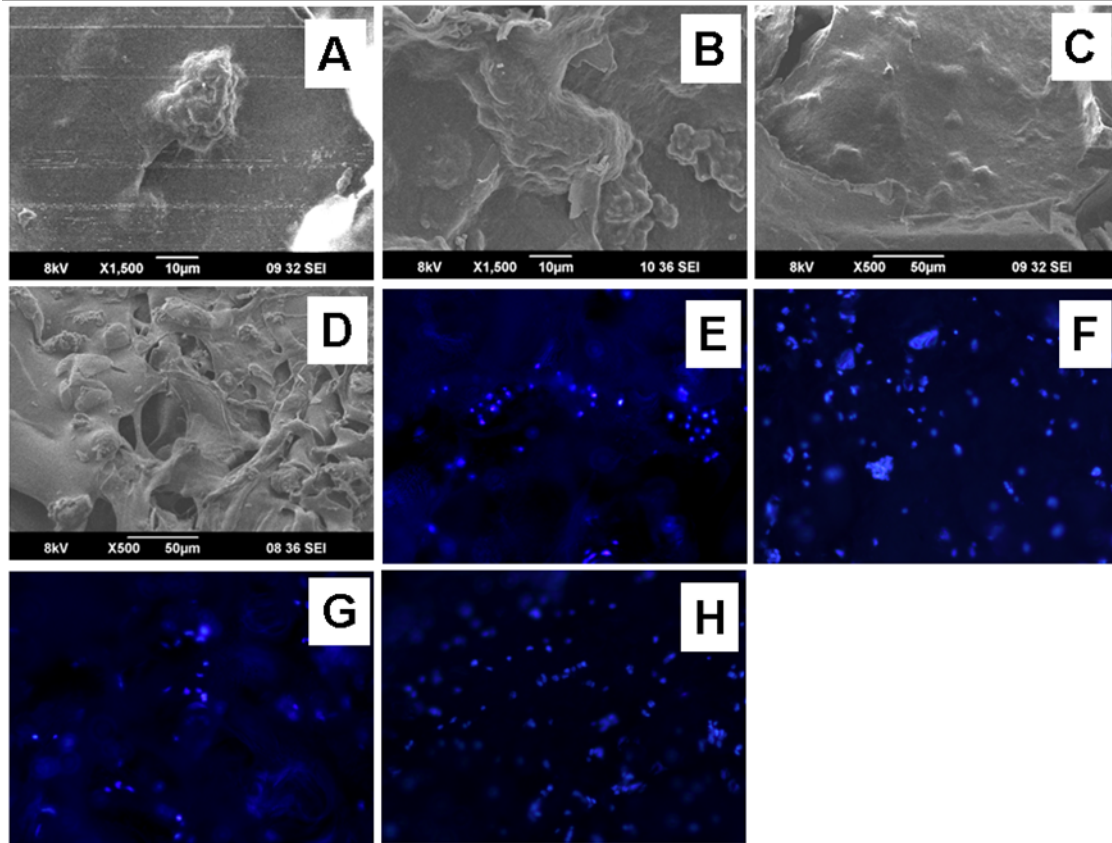

Figure 6: SEM images of cell attachment (12 hrs) of MG–63 cells on A. β–chitin scaffold (control) and B. β–chitin/nBGC composite scaffold, SEM images of cell attachment (12 hrs) of POB cells on C. β–chitin scaffold, D. β–chitin/nBGC composite scaffold. Fluorescent images of DAPI staining of MG–63 cells (12 hrs) on E. β–chitin scaffold (control) and F. β–chitin/nBGC composite scaffold, Fluorescent images of DAPI staining of POB cells (12 hrs) on G. β–chitin scaffold (control) and H. β–chitin/nBGC composite scaffold.

Figure 7: SEM images of cell proliferation (72 hrs) of MG–63 cells on A. β–chitin scaffold (control) and B. β–chitin/nBGC composite scaffold, SEM images of cell proliferation (72 hrs) of POB cells on C. β–chitin scaffold, D. β–chitin/nBGC composite scaffold. Fluorescent images of DAPI staining of MG–63 cells (72 hrs) on E. β–chitin scaffold (control) and F. β–chitin/nBGC composite scaffold, Fluorescent images of DAPI staining of POB cells (72 hrs) on G. β–chitin scaffold (control) and H. β–chitin/nBGC composite scaffold.

Cell Viability Studies

Cytocompatibility of β–chitin scaffold (control) and β–chitin/nBGC composite scaffolds were assessed using Alamar blue assay. The results suggest that there are no significant toxic leachables in the β–chitin/nBGC composite scaffolds compared to β–chitin control scaffolds (Fig.5A,B).

Cell Attachment Studies

SEM micrographs and DAPI staining were used to study the biocompatibility, attachment and morphology of MG–63 and POB cells on the β–chitin/nBGC composite scaffolds. The SEM images of cells incubated for 12 hrs on the scaffolds are seen (Fig.6A–D).

Fluorescent images of DAPI staining of cells incubated for 12 hrs on the composite scaffolds also revealed that cells were attached and distributed throughout the scaffold. More cells were attached on the β–chitin/nBGC composite scaffolds in comparison to the β–chitin control scaffolds. This indicates that the composite scaffolds showed enhanced biocompatibility than the control scaffolds (Fig.6E–H).

Cell Proliferation Studies

SEM micrographs and DAPI staining were used to study the proliferation and spreading of MG–63 and POB cells on the β–chitin/nBGC composite scaffolds. The images showed that MG–63 and POB cells proliferated over the entire surface area of the scaffolds (Fig.7A–D). The fluorescent images of DAPI staining of cells incubated for 72 hrs on the composite scaffolds also revealed that cells were well spread and distributed throughout the scaffold (Fig.7E–H). More cells were proliferated on the β–chitin/nBGC composite scaffolds in comparison to the β–chitin control scaffolds. This demonstrates that the composite scaffolds showed enhanced biocompatibility than the control scaffolds.

POB Maturation and Mineralization

The extent of POB maturation, matrix production and mineralization was assessed using SEM and EDS. The formation of mineralized bone nodules and calcium deposits were examined. Following osteoblast maturation and extracellular matrix production *in vitro*, mineralization of the matrix begins. After day 7 in culture, the formation of mineralized nodules was observed. Following 14 and 21 days in culture, very well defined mineralized nodules were observed. The SEM image of mineralised nodules in 7, 14 and 21 days respectively thus indicates enhanced matrix deposition and mineralization in the absence of osteogenic supplements [28] (Fig.8A–D). EDS spectra of mineralization showed the Ca/P ratio of 1.69 (Fig.8E). This result shows the bioactive nature of the composite scaffolds.
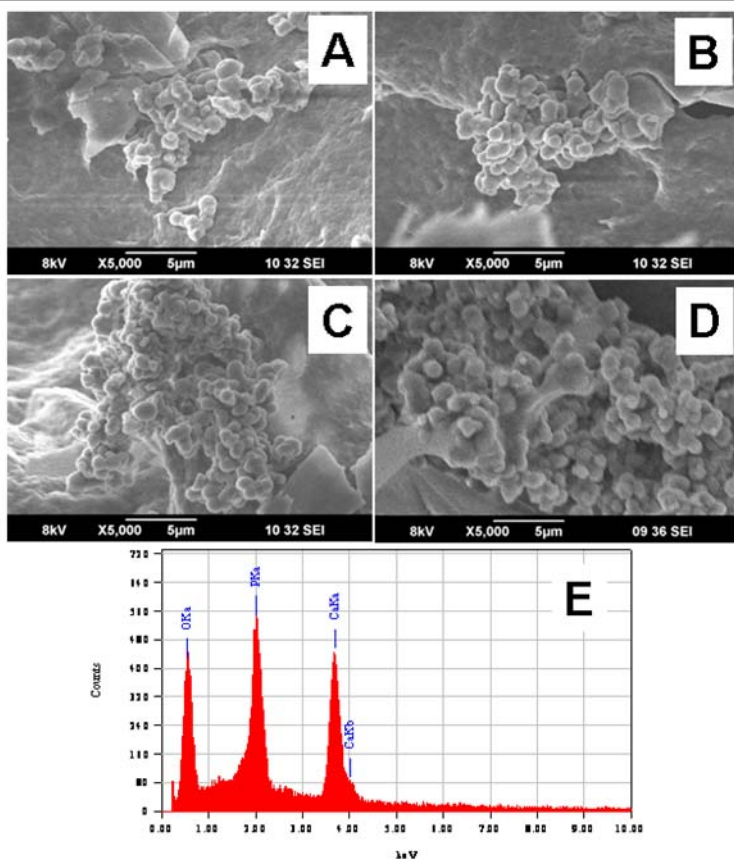
Figure 8: SEM images of mineralization due to POB differentiation on *β*–chitin/nBGC composite scaffold after A. 0, B. 7, C. 14 and D. 21 days. E. EDS spectra of mineralization due to POB differentiation on *β*–chitin/nBGC composite scaffold after 14 days.

Discussion

The nBGC particles obtained by sol–gel method were found to have size in the range of 50–150 nm and spherical shaped, indicating their stable nature. The sol–gel process allows one to obtain bioglasses of higher purity, surface area, and homogeneity than by the fusion method [19]. The pore size of the *β*–chitin/nBGC composite scaffold were determined by SEM analysis and was found to be in the range of 100–300 μm which is suitable for tissue engineering applications [3, 4, 7]. The pores were well interconnected and macroporous in nature. Pores are essential for adherence, proliferation and differentiation of osteoblasts. It also enhances the nutrient and oxygen supply and vascularisation. Relatively larger pores favour direct osteogenesis while smaller pores result in osteochondral ossification. The EDS spectrum of *β*–chitin/nBGC composite scaffold shows the peaks of Ca, P, Si and O. The atomic ratio of Si:Ca:P:O was found to be 29:13:8:48.

FTIR studies showed strong interaction between nBGC and *β*–chitin polysaccharide structure. The spectra of nBGC showed vibration bands at 467 and a shoulder at 1200cm^{-1} which are assigned to Si–O–Si bending mode. The vibration band at 1070cm^{-1} and a double peak at 607 and 567cm^{-1} are due to the stretching vibration of phosphate groups. The spectra of *β*–chitin scaffold indicate peaks at 1231 and 1748 cm^{-1} which correspond to C–O

and C=O stretching vibration modes of the amide group. The spectra of *β*–chitin/nBGC composite scaffolds showed the combined peaks of *β*–chitin and bioglass [29, 30].

The XRD spectra of the *β*–chitin/nBGC composite scaffold showed the peaks of *β*–chitin. The spectra of nBGC showed no diffraction peaks indicating the amorphous nature of nBGC [29–31].

In the thermogram, all the scaffolds showed decomposition in the range of 50–100°C which was due to the removal of physically adsorbed water. *β*–chitin control showed a second decomposition in the range of 270 to 350°C due to the decomposition of polysaccharide structure of *β*–chitin and all other scaffolds showed in the range of 270 to 370°C. The decomposition rates of the composite scaffolds were decreased slightly, due to the presence of nBGC [30].

The composite scaffolds showed lower swelling compared to control with the addition of nBGC due to the strong interaction of nBGC with the *β*–chitin structure. This is because the scaffolds with nBGC have lesser porosity compared to the control. Swelling and porosity aids in the supply of nutrients and oxygen to the interior regions of the composite scaffolds. It also increases the surface area allowing for cells to adhere to the surface of the composite scaffolds. However increase in swelling will also decrease the mechanical properties of the scaffold. Hence controlled

swelling will be ideal for tissue engineering applications [24, 31].

The degradation studies showed that the composite scaffolds are biodegradable. Hence, these composite scaffolds can be used for tissue engineering application. According to literature, an ideal scaffold should be biodegradable and rate of degradation should match the tissue regeneration [15, 25]. The β–1, 4–glycosidic linkage of chitin is susceptible to degradation by lysozyme. The degradation rate was significantly reduced with the addition of nBGC which may be due to neutralization of the acidic degradation products of β–chitin by the alkali groups leaching from nBGC, thus reducing the degradation rate of the scaffold. The leachable products of bioactive glass systems are known to be alkaline in nature [15].

The results of biomineralization studies showed the bioactive nature of the composite scaffolds thus suggesting that these scaffolds might be ideal for cells to deposit extra cellular matrix of bone composed of inorganic apatite that is beneficial in dental and orthopaedic applications. The mineral deposits were found to increase with increasing time of incubation which is clearly seen in the XRD, FTIR, EDS and SEM images. The EDS studies showed that the surface deposition was apatite with Ca/P ratio of 1.71. It is close to the theoretical value of 1.67 [15, 26].

Cell viability studies proved the non–toxic nature of composite scaffolds against MG–63 and POB cells. The cell viability was not affected by the addition of nBGC. The nBGC can cause alkalization of culture medium due to the leachable products from nBGC, which may lead to an increase in Ca^{2+} ions in culture medium thereby inducing apoptosis of the cells. However, our results indicate that there is no significant reduction in cell viability compared to the controls demonstrating that composite scaffolds are biocompatible [15]. This can be attributed to the confined nature of nBGC within the scaffold which will get released only slowly during the degradation.

Cell attachment and proliferation studies showed that MG–63 and POB cells were well attached and spread throughout the surface of the composite scaffolds. The scaffolds have shown to have excellent biocompatibility in terms of osteoblastic cells MG–63 and POB cultures. Initially rounded morphology of cells is seen during attachment followed by flattened well spread morphology of the cells on the scaffolds. The SEM images also indicated the formation of bridges between the pores. The higher attachment and proliferation on composite scaffolds may be due to increase in surface area and roughness of the surface. It is known that surface topology could play a role in cell attachment and proliferation on implants [32, 33]. Nano–surfaces have larger surface area to volume ratio offered by nBGC.

The extent of POB maturation, matrix production and mineralization was assessed using SEM and EDS. The formation of mineralized bone nodules and calcium deposits were noted. Following osteoblast maturation and extracellular matrix production *in vitro*, mineralization of the matrix begins. After day 7 in culture, the formation of mineralized nodules was observed. Following 14 and 21 days in culture, very well defined mineralized nodules were observed. The EDS studies showed that the surface deposition was apatite with Ca/P ratio of 1.69. It is close to the theoretical value of 1.67 [28]. Thus, the maturation and mineralization of the osteoblast cells in the absence of osteogenic supplements proved beneficial. Hence, the composite scaffold could be an ideal tissue engineering scaffold when implanted with cells for periodontal bone regeneration.

Conclusion

The β–chitin hydrogel/nBGC nano composite scaffolds prepared and characterized were found to have good material characteristics and ideal porosity for tissue engineering. Cell adherence and proliferation were found to be significantly improved on the composite scaffolds. Interestingly, the differentiation and mineralization of POB cells took place even in the absence of osteogenic supplements. Altogether, our results suggest that, this biocompatible and bioactive β–chitin hydrogel/nBGC composite scaffold could be ideal for regenerating periodontal bone in defects. Also, the scaffold can act as a bone filling material and as coating material for dental implants.

Acknowledgements

References

1. T. Chang, Q. Liu, V. Marino and P.M. Bartold, Attachment of periodontal fibroblasts to barrier membranes coated with platelet–rich plasma, Aust. Dent. J., 52, 227–233 (2007).
2. A. H. Melcher and J. E. Eastoe, The connective tissues of the periodontium, In: A.H. Melcher and W.H. Bowen (eds.), Biology of the periodontium, Academic Press, New York, 167–343 (1969).
3. D. M. Williams, F. J. Hughes, E. W. Odell and P. M. Farthing, The normal periodontium, In: Pathology of periodontal diseases, Oxford university press, New York, 17–30 (1992).
4. B. Zhang, X. J. Zhang, C. Y. Bao, Q. Wang, J. F.Yao, H. S. Fan, C. D. Xiong, X. D. Zhang, Repairing periodontal bone defect with in vivo tissue engineering bone, Key Eng. Mater., 330, 1121–1124 (2007).
5. M. A. Reynolds, M. E. Aichelmann–Reidy and G.L. Branch–Mays, Regeneration of periodontal tissue: bone replacement grafts, Dent. Clin. N Am., 54, 55–71 (2010).
6. S. V. Dorozhkin, Nanosized and nanocrystalline calcium orthophosphates, Acta Biomaterialia, 6, 715–734 (2010).
7. J. L. Karen, Burg, S. Porter and F. K. James, Biomaterial developments for bone tissue engineering, Biomaterials, 21, 2347–2359 (2004).

8. I. Y. Kim, S. J. Seo, Moon, M. K. Yoo, I. Y. Park, B.C. Kim and C. S. Cho, Chitosan and its derivatives for tissue engineering applications, Biotechnol. Adv., 26, 1–21 (2008).

9. H. Tamura, T. Furuike, S. V. Nair and R. Jayakumar, Biomedical applications of chitin hydrogel membranes and scaffolds, Carbohyd. Polym., DOI : 10.1016/j.carbpol.2010.06.001.

10. R. Jayakumar, M. Deepthy, K. Manzoor, S.V. Nair and H. Tamura, Biomedical applications of chitin and chitosan based nanomaterials–A short review, Cabohydr. Polym., 82, 227–232 (2010).

11. S. Hirano, Chitin and chitosan as novel biotechnological materials, Ullmanns Encyc. Ind. Chem. A., 6, 231–238 (1986).

12. K. S. Chow, E. Khor and A. C. A. Wan, Porous chitin matrices for tissue engineering: fabrication and in–vitro cytotoxic assessment, J. Polym. Res., 8, 27–35 (2001).

13. H. Tan and G. M. Kacey, Injectable biodegradable hydrogels for tissue engineering applications, Materials, 3, 1746–1767 (2010).

14. R. A. A. Muzzarelli and C. Muzzarelli, Chitosan Chemistry: Relevance to the Biomedical Sciences, Adv. Polym. Sci., 186, 151–209 (2005).

15. P. Mathew, P. T. Sudheesh Kumar, N. S. Binulal, S. V. Nair, H. Tamura and R. Jayakumar, Development of novel β–chitin/nanobioactive glass ceramic composite scaffolds for tissue engineering applications, Carbohydr. Polym., 78, 926–931 (2009).

16. G. Philippe, V. Laurent, D. Jacques and D. Alain, Study of a chitin–based gel as injectable material in periodontal surgery, Biomaterials, 23, 1295–1302 (2002).

17. H. Tamura, H. Nagahama and S. Tokura, Preparation of chitin hydrogel under mild conditions, Cellulose, 13, 357–364 (2006).

18. L. L. Hench, R. J. Splinter, W. C. Allen and T. K. Jr Greenlee, Bonding mechanism at interface of ceramic prosthetic materials, J. Biomed. Mater. Res. Symp., 2,117–141 (1971).

19. J. Roman, S. Padilla and M. Vallet–Regý, Sol–Gel Glasses as Precursors of Bioactive Glass Ceramics, Chem. Mater., 15, 798–806 (2003).

20. D. A. Jones, Principles and Prevention of Corrosion, MacMillan Publishing Company Singapore, 9,213 (1992).

21. C. Marta, M. Giuliana, B. Vera and M. Claudio, Characterization of sol–gel bioglasses with the use of simple model systems: a surface–chemistry approach, J. Mater. Chem., 13, 1279–1286 (2003).

22. A. Oliva, A. Salerno, B. Locardi, V. Riccio, R.F. Della, P. Iardino and V. Zappia, Behaviour of human osteoblasts cultured on bioactive glass coatings, Biomaterials, 19, 1019–1025 (1998).

23. S. Foppiano, S. J. Marshall, G. W. Marshall, E. Saiz and A. P. Tomsia, Bioactive glass coatings affect the behaviour of osteoblast–like cells, Acta Biomaterialia, 3, 765–771 (2007).

24. A. Liu, Z. Hong, X. Zhuang, X. Chen, Y. Cui, Y. Liu and Y. Jing. Surface modification of bioactive glass nanoparticles and the mechanical and biological properties of poly(L–lactide) composites, Acta Biomaterialia, 4, 1005–1015 (2008).

25. L. Jiang, Y. Li and X. Chengdong, Preparation and biological properties of a novel composite scaffold of nano–hydroxyapatite/chitosan/carboxymethyl cellulose for bone tissue engineering, J. Biomed. Sci., 16, 65 (2009).

26. P. Mathew, N .S. Binulal, S. V. Nair, N. Selvamurugan, H. Tamura and R. Jayakumar, Novel biodegradable chitosan–gelatin/nano–bioactive glass ceramic composite scaffolds for alveolar bone tissue engineering, Chem. Eng. J., 158, 353–361 (2010).

27. T. Kokubo and H. Takadama, How useful is SBF in predicting in–vivo bone activity, Biomaterials, 27, 2907–2915 (2006).

28. T. Olga, R. J. Julian, M. P. Julia and M. S. Molly, Differentiation of fetal osteoblasts and formation of mineralized bone nodules by 45S5 Bioglass conditioned medium in the absence of osteogenic supplements, Biomaterials, 30, 3542–3550 (2009).

29. H. Kong and J. Jang, One–step fabrication of silver nanoparticles embedded polymer nanofibers by radical–mediated dispersion polymerization, Chem. Commun., 28, 3010–3012 (2006).

30. S. Petrova, S. Miloshev, R. Mateva and I. Illev, Synthesis of amphiphilic PEG–PCL–PEG triblock copolymer, J. Univ. Chem. Technol. Metall., 43, 199–204 (2008).

31. R. Marguerite, Chitin and chitosan: Properties and applications, Prog. Polym. Sci., 31, 603–632 (2006).

32. P. Gowsihan, I. Claudia, T. Olga, M. Muthu, G. H. Robert, M. S. Molly, V. H. John, E. S. Mark and J. R. Jones, Synthesis of bioactive class II poly(γ–glutamic acid)/silica hybrids for bone regeneration, J. Mater. Chem., 20, 8952–8961 (2010).

33. M. D. O'Donnell, P. L. Candarlioglu, C. A. Miller, E. Gentlemanc and M. M. Stevens, Materials characterisation and cytotoxic assessment of strontium–substituted bioactive glasses for bone regeneration, J. Mater. Chem., 20, 8934–8941 (2010).